Design of Triple-Active Bridge Converter with Inherently Decoupled Power Flows

Dong-Uk Kim, ByengJoo Byen, ByungHwang Jeong, and Sungmin Kim
Hanyang University, Hyosung Corporation
Ansan, Anyang, Korea
Tel.: +82/31-400-5172.
E-Mail: ksminmoon@hanyang.ac.kr

Keywords

«DC-DC converter», «Tri-port isolated converter», «Bi-directional converters», «Efficiency», «Design».

Abstract

For the realization of DC grid, the high-power multi-port isolated DC/DC converter is necessary to integrate various DC sources and loads. Triple-Active Bridge (TAB) converter is one of the most popular topologies which has three-port high frequency transformer and three active bridges. It can realize the bi-directional power flow among different sources and loads. However, the intrinsic power coupling in each port of three-port transformer leads to the unwanted voltage fluctuation of DC side. The power coupling among three ports can be minimized by a low leakage inductance at one port. However, it can decrease the power efficiency in some power flow conditions of TAB converter. This paper has analyzed the reason for the degradation of power efficiency in various power flow condition. To estimate the power loss components in TAB converter, the power loss breakdown method is used. With the two experimental configuration of TAB converter: the conventional leakage inductance and a low leakage inductance, the power loss is estimated. From the experimental results, it can be concluded that the designing method of leakage inductance with a low leakage inductance at one port is appropriate for the TAB converter which has fixed power flow condition.

Introduction

As the increasing demand on DC power, the high-power DC-DC converter which can combine various DC sources/loads has been developed. For the integration of various DC sources/loads, a Triple-Active Bridge (TAB) converter is an appropriate candidate for its 3-way and bi-directional power control [1]. The TAB converter controls the power via three-port High Frequency Transformer (HFT). At each port, various type of DC sources/loads can be connected with half or full-bridge converters. The power flow of TAB converter can be controlled by adjusting the phase of three port voltages. Generally, the phase of one port is fixed and those of the others are shifted. Therefore, TAB converter has two controllable phase shift angles to control three port power. However, TAB converter has a coupled power among three ports since the three ports of HFT have magnetically coupled structure. It makes an intrinsic power coupling of three ports. This power coupling always exists in multi-port high frequency transformer. Therefore, it is hard to control each port power independently. In previous studies, various decoupling control algorithms are suggested to minimize the effect of power coupling [2],[3]. However, these algorithms are complicated to be applied, and the decoupling performance is definitely dependent on the inductance values of the TAB converter. Moreover, the system parameters are not easy to recognize exactly. As another approach, the decoupling method that uses a low leakage inductance at one port of HFT is suggested in [4]. With a low leakage inductance at one port, the power flows between the other ports are minimized. This method requires only two external series inductors for customizing the phase shift angle guaranteeing the confident decoupling performance with no complex control algorithm. In addition, the size and cost of magnetic components can be saved. However, the total loss

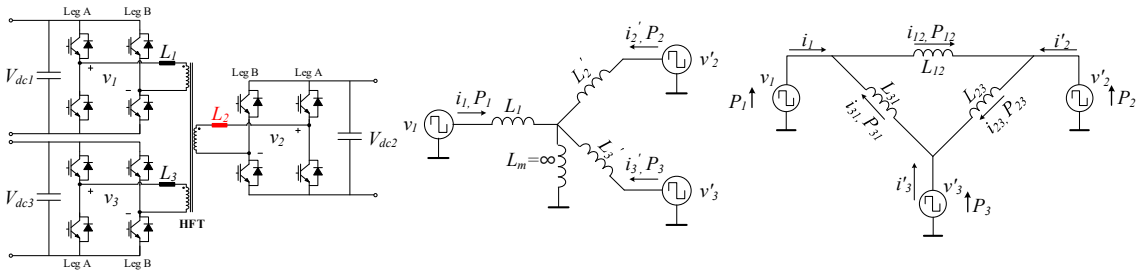

Fig. 1: Triple active bridge converter (a) schematic (b) Wye-model (b) Delta-model

of TAB converter can be increased due to the high peak current at the low leakage inductance port. Therefore, the careful design of leakage inductance and configuration is required.

In this paper, the brief review of TAB converter according to the leakage inductance is described. Then, the two methods designing leakage inductance are suggested: the conventional three leakage inductances configuration and the two leakage inductances with a low leakage inductance. The efficiencies of two cases are compared in various power flow condition and the reason for efficiency degradation is analyzed. Using the power loss breakdown method, each power loss component is estimated in various power condition. In addition, the guideline for selecting the position of low leakage port guaranteeing the decoupled power control and high efficiency is suggested. To verify the analysis and design methods, the experiments with 2kW TAB converter are conducted.

TAB converter with a low leakage inductance at one port

The schematic of TAB converter can be seen in Fig. 1(a). Each port of HFT consists of leakage inductance and full-bridge converter. The leakage inductance, L_1, L_2, L_3 includes the intrinsic leakage inductance of HFT, $L_{\sigma 1}$, $L_{\sigma 2}$, $L_{\sigma 3}$, and the external series inductance, L_{s1}, L_{s2}, L_{s3}. To control the power flow of each port, two controllable phase shift angles of port voltage, ϕ_{12}, ϕ_{13} are used. The phase shift angle of port-1 voltage is fixed to zero, and ϕ_{12}, ϕ_{13} are shifted. Fig. 1(b) shows the Wye-model of TAB converter. The voltage, current, inductances are referred to the port-1 side. To analyze the power transfer between two ports, Delta-model is used as shown in Fig. 1(c). The inductors, L_{12}, L_{23}, L_{31} are equivalent leakage inductance between two ports in Delta-model. The power delivered between two ports via equivalent leakage inductance of Delta-model, P_{12}, P_{23}, P_{31} can be derived as follows [5]:

$$\begin{cases} P_{12} = \dfrac{V_1 V_2'}{2\pi^2 f_{sw} L_{12}} \phi_{12}(\pi - \phi_{12}) \\ P_{23} = \dfrac{V_2 V_3'}{2\pi^2 f_{sw} L_{23}} \phi_{23}(\pi + \phi_{23}) \\ P_{31} = -\dfrac{V_1 V_3'}{2\pi^2 f_{sw} L_{31}} (\phi_{23} + \phi_{12})(\pi - (\phi_{23} + \phi_{12})) \end{cases} \quad (1)$$

Through (1), the port power from each port can be derived as follows:

$$P_1 = P_{12} - P_{31},\ P_2 = -P_{12} + P_{23},\ P_3 = P_{31} - P_{23} \quad (2)$$

In (2), two phase shift angles determine port power. It means that the control loops that controls each port power cannot be configured independently. The control loops have inherent coupling term, and it is configured in Two Input Two Output (TITO) form. The input parameters are two phase shift angle, and output parameters are two port power. The decoupling control methods have been studied in many papers to control in Single Input Single Output (SISO) form. Recently, a method has been proposed to minimize the power decoupling between two output power through the design of component values, not algorithm: One inductance is designed to be very small and other two inductance to be proper values to transfer the power among three ports. If the leakage inductance at port-2 is very low ($L_2 \approx 0$), the equivalent leakage inductance can be simplified as follows:

$$L_{12} = L_1 + L_2' + \frac{L_1 L_2'}{L_3'} \approx L_1,\ L_{31} = L_1 + L_3' + \frac{L_1 L_3'}{L_2'} \approx \infty,\ L_{23} = L_2' + L_3' + \frac{L_2' L_3'}{L_1} \approx L_3' \quad (3)$$

By the simplified equivalent inductance, the power transfer between the port-1 and port-3, P_{31} is almost zero even though phase shift angle ϕ_{12}, ϕ_{13} are varying. Therefore, the power from each port can be simplified as follows:

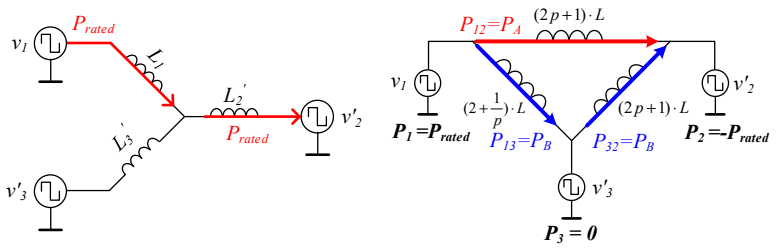

Fig. 2: The power flow in case of $P_1 = -P_2$ and $L_1=L'_2=L'_3$ (a) in Y-model (b) in Delta-model

$$P_1 = P_{12},\ P_2 = -P_{12} + P_{23},\ P_3 = -P_{23} \tag{4}$$

From (1) and (4), the port-1 power, P_1 is controlled by only ϕ_{12} and the port-3 power, P_3 is controlled by ϕ_{23}, independently. Therefore, two control loops that controls the power of each port can be configured in SISO form. This method guarantees the confident decoupling performance with no complex control algorithm. In addition, the external series inductor is not necessary to customize the phase shift angle. However, the power efficiency can be decreased in some power flow conditions due to the high peak current at the low leakage inductance port.

Design of Leakage inductance with a low leakage inductance at one port

In practical, the leakage inductance cannot be zero. In this paper, p is the ratio of a low leakage inductance to inductance of other ports. And the low leakage inductance is positioned at port-2. The leakage inductances can be defined as follows:

$$L_1 = L, L_2' = p \cdot L, L_3' = L \tag{5}$$

The equivalent leakage inductance can be calculated as (6).

$$L_{12} = \frac{L_1L_2'+L_2'L_3'+L_3'L_1}{L_3'} = (2p+1)L, L_{23} = \frac{L_1L_2'+L_2'L_3'+L_3'L_1}{L_1} = (2p+1)L, L_{13} = \frac{L_1L_2'+L_2'L_3'+L_3'L_1}{L_2'} = \left(2+\frac{1}{p}\right)L \tag{6}$$

In case of the bi-directional TAB converter, it can have various power flow conditions. Therefore, the leakage inductance should be designed considering these various power flow conditions. In general, the inductance should be designed enough to transfer the rated power between the interfacing active bridge ports.

In following design procedure, it is assumed that the rated power is delivered from port-1 to port-2 as shown in Fig. 2. In Wye-model, the rated power, P_{rated} is delivered via L_1 and L_2. In Delta-model, the power from port-1 is divided into two power terms (P_A and P_B) according to the impedance of equivalent inductance. In this condition, the active power delivered by port-3 is zero, and P_{13} is same with P_{32}. Therefore, power terms in Delta-model can be determined as follows:

$$P_A + P_B = P_{rated} \tag{7}$$

$$P_A = \frac{2p+\frac{1}{p}+3}{4p+\frac{1}{p}+4} \cdot P_{rated}, P_B = \frac{2p+1}{4p+\frac{1}{p}+4} \cdot P_{rated}\ . \tag{8}$$

Assuming the maximum phase shift angle, $\phi_{12,max}$, the P_A is delivered and the power equation is as follows:

$$P_A = \frac{V_1V_2'}{2\pi^2 f_{sw}L_{12}}\phi_{12,max}(\pi - \phi_{12,max}) \tag{9}$$

From (6), (8) and (9), the maximum value of L in (5), L_{max} can be derived.

$$L_{max} = \frac{K}{(2p+1)\cdot P_{rated}} \cdot \frac{4p+\frac{1}{p}+4}{2p+\frac{1}{p}+3} \qquad \left(K = \frac{V_1V_2'}{2\pi^2 f_{sw}}\phi_{12,max}(\pi - \phi_{12,max})\right) \tag{10}$$

In the conventional three inductance design, the ratio, p is designed to be 1. Three active bridge ports in TAB converter have same leakage inductance. The maximum leakage inductance and equivalent leakage inductance are (11) and (12), respectively.

$$L_{\max,p=1} = \frac{1}{2} \cdot \frac{K}{P_{rated}} \tag{11}$$

$$L_{12} = L_{23} = L_{31} = 3 \cdot L_{max,p=1} \tag{12}$$

In the two-leakage inductance design with a low inductance at one port, the ratio, p is designed to be very small value such as 0.05, which is the only 5% of other two leakage inductance values. The maximum leakage inductance and equivalent leakage inductance are (13) and (14), respectively.

$$L_{max,p=0.05} \approx 0.95 \cdot \frac{K}{P_{rated}} \tag{13}$$

$$L_{12} = L_{23} = 1.1 \cdot L_{max,p=0.05},\ \ L_{13} = 22 \cdot L_{max,p=0.05} \tag{14}$$

Power loss analysis of TAB converter in various power flow path

A. Variation of peak current according to the configuration of leakage inductance

The current waveforms of each port can be determined by the leakage inductance and the phase shift angle. Especially, the peak current of active port having a low leakage inductance can be significantly increased in some power flow conditions. The increased peak current leads to the increase of power loss components which are related to the peak current. To predict the power loss variation according to the leakage inductance, the peak current value is expected by deriving the current equation. Among various power flow conditions, the two cases are analyzed, and the peak current value is compared.

Fig. 3 shows power flow diagrams in Delta-model and steady-state waveforms in case of P_1=-P_3. In this case, the relationship of phase shift angle is $\phi_{21}<0$, $\phi_{23}>0$. Therefore, the power is delivered from port-1 to port-3. When the leakage inductance of all ports exists as shown in Fig.3(a), which is p=1, the power transferred via L_{12} is as follows:

$$P_{12,p=1} = \frac{1}{3} P_{rated} = \frac{V_1 V_2'}{2\pi^2 f_{sw} L_{12}} \phi_{12,p=1}. \tag{16}$$

When the leakage inductance at port-2 is very low as shown in Fig. 3(b), which means p is nearly 0, the power transferred via L_{12} is as follows:

$$P_{12,p=0} = P_{rated} = \frac{V_1 V_2'}{2\pi^2 f_{sw} L_{12}} \phi_{12,p=0}. \tag{17}$$

From (16) and (17), the relationship of phase shift angle in two cases can be obtained.

$$\phi_{12,p=0} = 2 \cdot \phi_{12,p=1} \tag{18}$$

Using (18), the peak current value at the port-2 where the active power is not delivered can be calculated as follows:

$$i_{2,p=1}(t_1) = \frac{2V_1}{2\pi f_{sw} L_{23}} \phi_{12,p=1} \tag{19}$$

$$i_{2,p=0}(t_1) = \frac{6V_1}{2\pi f_{sw} L_{23}} \phi_{12,p=1} \tag{20}$$

In case of using low leakage inductance at one port, the peak current at low leakage inductance port increase three times as obtained in (20). As shown in Fig. 3(c), the phase shift angle and peak current relationship are verified in simulation results. In this case, the peak current significantly increases, which is the reason for high turn-off switching loss in full-bridge converter at port-2. On the other hand, due to the absence of external series inductance, $L_{2,series}$, the core and copper loss of inductor does not exists. However, the increase of switching loss at low leakage inductance side is large enough to degrade the power efficiency of TAB converter.

In Fig.4, the power is delivered from port-1 and 3 to port-2, equally. In this case, the relationship of phase shift angle can be calculated as same procedure with (16)-(18).

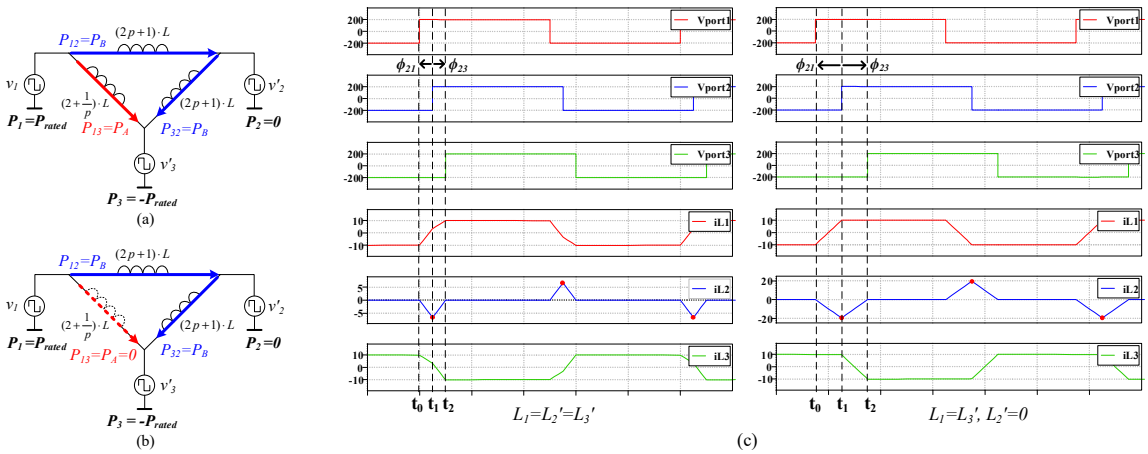

Fig. 3: Power flow of TAB converter in case of P_1=-P_3 (a) L_1=L'_2=L'_3 (b) L_1=L'_3, $L'_2\approx 0$ (c) current and voltage waveforms

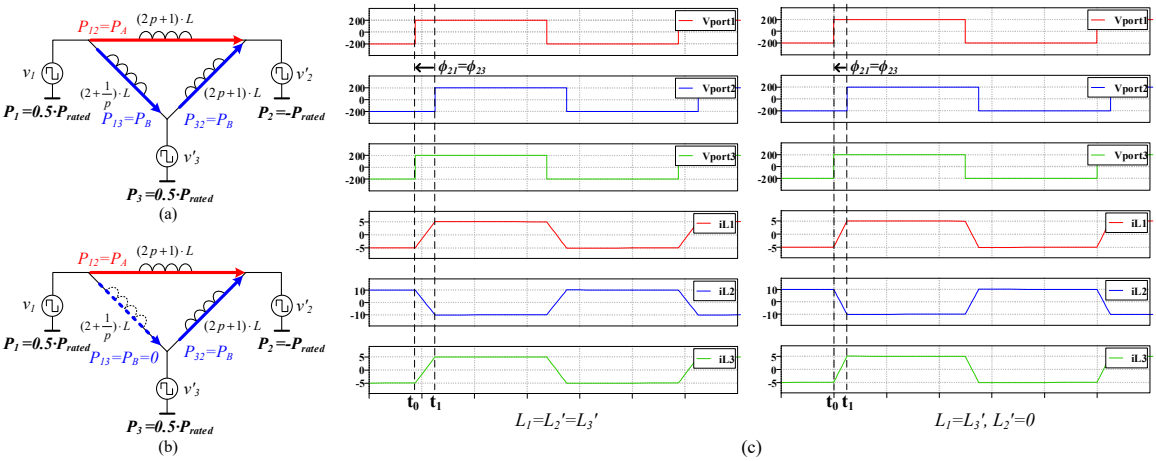

Fig. 4: Power flow of TAB converter in case of P_1=P_3=0.5·P_{rated}, P_2=-P_{rated} (a) L_1=L'_2=L'_3 (b) L_1=L'_3, $L'_2\approx 0$ (c) current and voltage waveforms

$$\phi_{12,p=0} = \frac{2}{3}\phi_{12,p=1} \tag{21}$$

Using (21), the peak current value at the port-2 where the low leakage inductance side can be calculated as follows:

$$i_{1,p=0}(t_1) = i_{1,p=1}(t_1) = \frac{V_1}{L_{12}\omega}\phi_{21}. \tag{22}$$

In this power flow condition, the peak current is same as calculated in (22). It can be concluded that the turn-off switching loss of full-bridge converter at port-2 is also same. In addition, due to the absence of external series inductance of port-2, the inductor core and copper losses does not exist. As a result, the total power loss can be reduced. The results of two power flow in Fig. 3 and 4 show that the peak current increases in some power flow condition and the switching loss can be also increases, which can affect to the total power efficiency. Therefore, the position of a low leakage inductance should be carefully selected. To analyze the effect of variation of peak current to the power loss of TAB converter, the power loss breakdown is conducted in next section.

B. Power loss breakdown procedure of TAB converter

In this section, the power loss breakdown method is used for TAB converter. There are many previous studies about the method of power loss breakdown for the DC/DC converter [6]-[9]. In the DC/DC converter such as TAB converter, there are three main power loss components: 1) power devices, 2) high-frequency transformer 3) series inductors. In this paper, it is assumed that the leakage inductances

of transformer of three ports are minimized. The leakage inductance which is necessary for delivering power is realized by connecting additional series inductors. The power losses in controller and gate drivers are excluded in this case.

The power loss of power devices is composed of conduction loss, P_{cond} and switching loss, P_{sw}. The total conduction loss of the three full-bridge converter of TAB converter is calculated as follows:

$$P_{cond} = 4 \cdot R_{on} I_{1,rms}^2 + 4 \cdot R_{on} I_{2,rms}^2 + 4 \cdot R_{on} I_{3,rms}^2 \tag{23}$$

where R_{on} is on-state resistance of power device. The switching loss of power device occurs during turn-on and off state. The switching loss is proportional to the current flowing through the switch at the time of switching. In case of TAB converter, Zero-Voltage Switching (ZVS) enables the nearly zero switching loss during turn-on of switch. However, the DC/DC converter that uses phase-shift modulation suffer from the high-peak current during turn-off of switch. Therefore, the switching loss can be calculated as follows:

$$P_{sw} = P_{sw,Turn-on} + P_{sw,Turn-off} \approx P_{sw,Turn-off}. \tag{24}$$

In many manufactures of power device, the switching loss information according to the switch current and power loss models are supported. The switching loss can be easily obtained even with various power flow condition.

The power loss of transformer is determined by the winding loss and iron loss. The copper loss of winding is winding loss, $P_{wire,TR}$ and the winding loss of TAB converter can be calculated as follows:

$$P_{wire,TR} = R_{wire,1} I_{RMS,1}^2 + R_{wire,2} I_{RMS,2}^2 + R_{wire,3} I_{RMS,3}^2 \tag{25}$$

where $R_{wire,1}$, $R_{wire,2}$, and $R_{wire,3}$ are winding DC resistances of each port at TAB converter. In case of iron loss, it is determined by the electro-magnetic force and magnetization current of high-frequency transformer. Since these values are constant even different power flow condition, the iron loss of high-frequency transformer also has constant value. By injecting magnetization current at one port of high-frequency transformer, the iron loss can be measured experimentally.

The power loss of series inductor is similar with the that of high-frequency transformer: winding and iron loss. The winding loss of series inductor is calculated as follows:

$$P_{wire,L} = R_{wire,L} I_{RMS,L}^2 \tag{26}$$

where $R_{wire,L}$ is winding DC resistance of series inductor. The iron loss of inductor can be estimated by the Steinmetz equation, or the datasheet of core provided by the manufacturer.

$$P_L = K \cdot f^a \cdot B_{peak}^b \tag{27}$$

where K, a, and b are Steinmetz coefficient of the core, f is switching frequency, and B_{peak} is peak value of magnetic flux density. The peak magnetic flux density is calculated based on the peak inductor current value which is obtained experimentally and the B-H curve of the core. Using the described power loss breakdown method, the comparison of power losses with two leakage inductances configuration and three leakage inductances configuration are analyzed with experimental results in next section.

Experimental results

To verify the proposed method, the TAB converter setup is configured as shown in Fig. 5. To compare the power efficiency according to the leakage inductance, two different cases are set: the ratio, p=1 and p=0.01. First, the leakage inductance of all ports is equal (L_1=L'_2=L'_3=52uH), which is p=1. Second, the leakage inductance at port-2 is minimized (L_1=L'_3=104uH, L'_2=1uH), which is p=0.01. The output power of each port is controlled to the power reference of controller. The TAB converter is operated in six modes as shown in Fig. 5 to consider the various application of TAB converter. The power efficiency is experimentally measured using Newtons4th PPA4530 power analyzer. Each component of power loss is calculated based on the described power loss breakdown method.

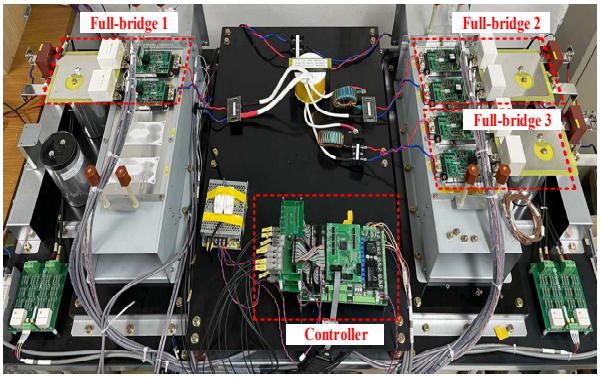

Fig. 5: TAB converter setup for experiment

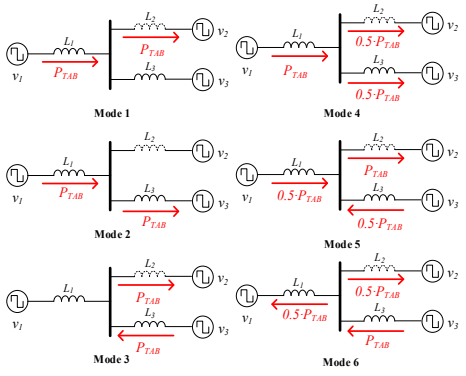

Fig. 6: six-operation mode of TAB converter

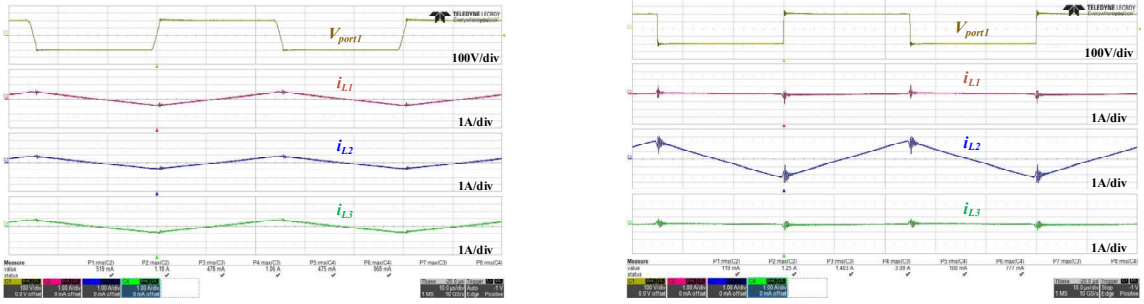

(a) (b)

Fig. 7: Steady-state voltage and current waveforms in no-load condition (a) p=1 (b) p=0.01

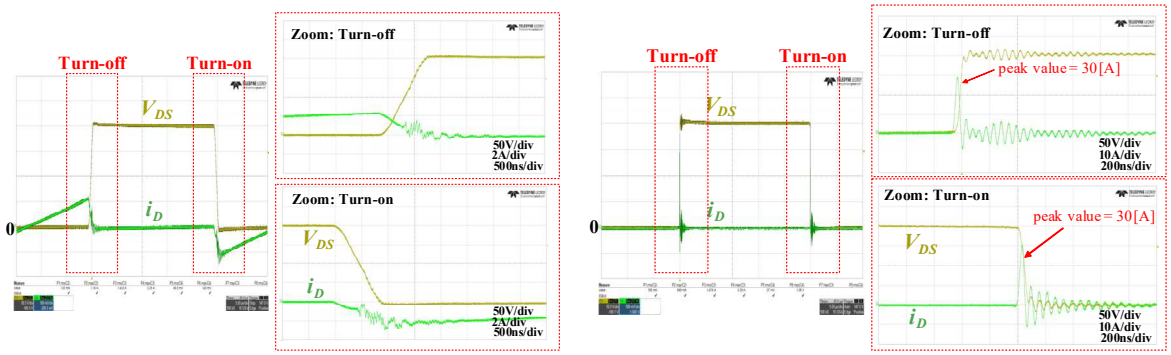

(a) (b)

Fig. 8: MOSFET drain-source voltage (V_{DS}) and drain current (i_D) waveforms in case of p=0.01 (a) upper switch of leg A at port-2 (b) upper switch of leg A at port-1

A. No-load condition

Fig. 7 shows the output voltage of port-1 and three port currents. In no load condition, the port currents are magnetization current. In case of p=1, the same magnitude of current flows to the three-port due to the equal leakage inductance distribution and the power loss is 10.4W. On the other hand, in case of p=0.01, most of the magnetization current is provided from the port-2 in which a low leakage inductance is located, and the power loss is 31.8W. The increase of power loss in case of p=0.01 is due to the current imbalance of three-port. The current imbalance of three-port during No-load condition can lead to the increase of switching loss. As shown in Fig. 7(b), the magnetization current is provided from the port-2 where the low leakage inductance is located. Fig. 8(a) and (b) show the drain-source voltage and drain current during turn-on and off of MOSFET in case of p=0.01. The drain current of switch is measured using Rogowski coil. The switch at port-2 satisfies the ZVS condition as shown in Fig. 8(a). However, in case of switch at port-1, the hard-switching occurs during turn-on because the current flowing through the switch is not enough to satisfy ZVS condition as shown in Fig. 7(b). In addition, as shown in Fig. 8(b), the current oscillation with high peak current during turn-on and off leads to the high turn-on and

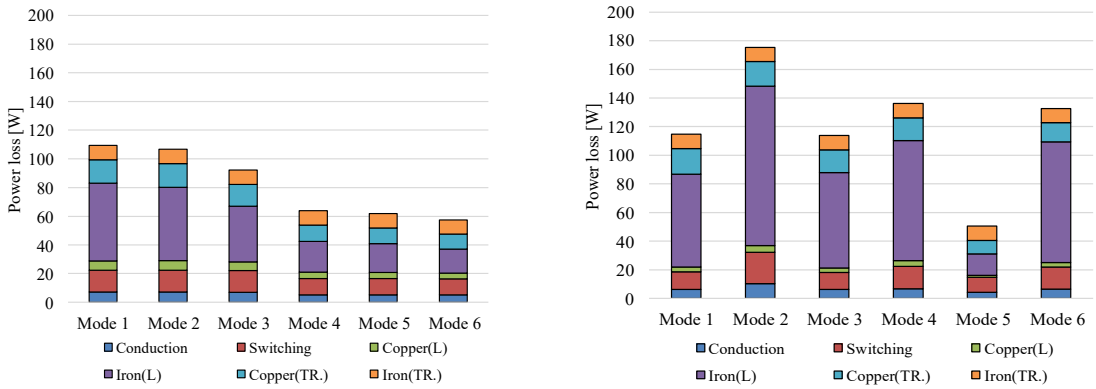

(a) (b)

Fig.9: Estimated power loss distribution at P_{TAB}=2kW (a) same leakage inductance at three-port (b) a low leakage inductance at one-port

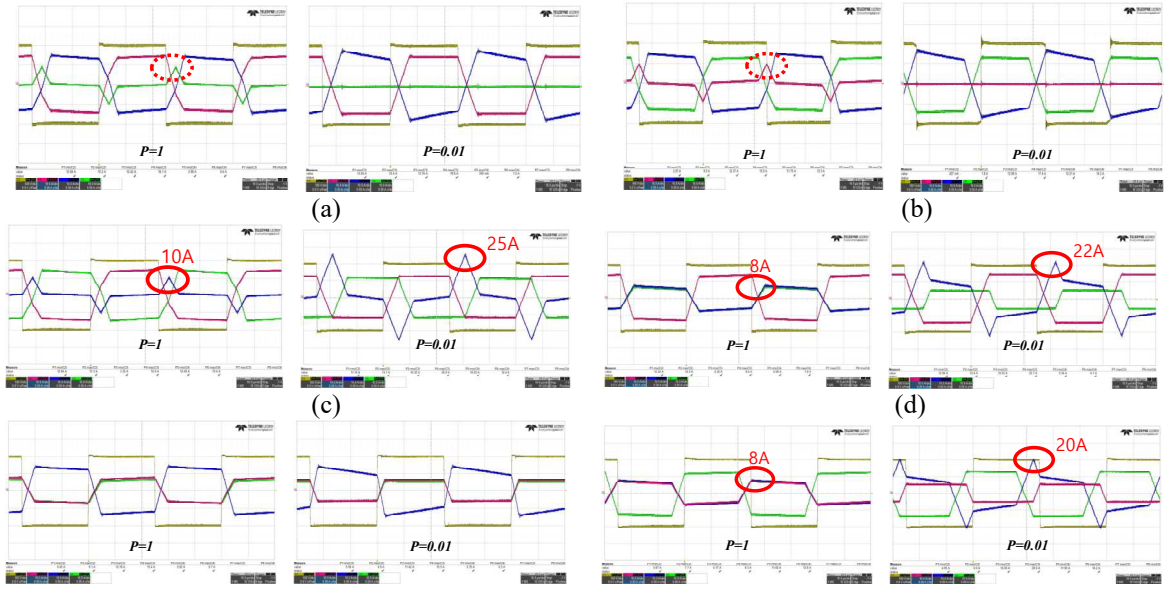

(a) (b) (c) (d) (e) (f)

Fig. 10: Steady-state waveform of TAB converter at *p=1* and *p=0.01*
(a) Mode 1 (b) Mode 2 (c) Mode 3 (d) Mode 4 (e) Mode 5 (f) Mode 6

off switching losses. Even though the power losses in series inductors and winding losses of port-1 and port-3 is reduced, the increase of switching losses is dominant. Eventually, it degrades the power efficiency of TAB converter with low leakage inductance at one port during No-load condition.

B. Six operation mode condition

To analyze the difference of power loss in various power flow condition, the six-operation modes are set, and the power losses are measured. The power loss breakdown method suggested in previous section is used to analyze the power loss components. Fig. 9 (a) and (b) represent the estimated power loss distribution at P_{TAB}=2kW in different leakage inductance configurations. Except the operation Mode 5, the power losses of two leakage inductances configuration are larger than those of three leakage inductances configuration. The major reason is that the peak current of inductor is increased due to the uneven leakage inductance distribution. As expected in (21) and (22), the peak current is equal in both case (*p=1* and *p=0.01*) and can be checked in Fig. 10(e). Therefore, the switching loss is same. Instead, the phase-shift angle is decreased in the case of p=0.01 as expected in (21) so that the conduction loss is slightly decreased. In addition, the elimination of series inductor at port-2, where the rated current flows, results in the significant power loss reduction in series inductors. With the low leakage inductance at port-2 (p=0.01), the power efficiency at Mode 5 is increased to 97.6% at P_{TAB}=2kW, which is a 1% increase from the case of evenly distributed leakage inductance (p=1). In the Mode 1, the equivalent

leakage inductance, L_{31} is infinite if the leakage inductance at port-2 is zero. Therefore, the current at L_{31}, i_{31} is also zero, which results in the ideally zero switching loss at port-3. However, the core loss and winding loss at port-2 are increased as shown in Fig. 9 because the leakage inductance is doubled ($L_{1,p=0.01}=L'_{3,p=0.01}=2 \cdot L_{1,p=1}=2 \cdot L'_{3,p=1}$). In case of Mode 3, the power flow is similar with the Mode 1 since the same leakage inductance at port-1 and port-3. Therefore, the power efficiency of Mode 1 and Mode 3 is estimated as same value. The operation mode 2, 4, and 6 are cases where the power delivered through the port with a low leakage inductance is below the half of the rated power. Due to the low leakage inductance, the *di/dt* of inductor current increases so that the peak current at the port also increases at the time of turn-off as shown in Fig. 10(c).

The power loss analysis of TAB converter in six operation modes shows that the effect of power loss reduction is valid only in mode 5. Therefore, it can be concluded that the proposed two leakage inductances configuration is appropriate for the TAB converter which has fixed power flow condition. In addition, to minimize the power losses and utilize the power decoupling, the low leakage inductance should be located at the port that the most active power is transferred. If the power flow of the three ports of the TAB converter is not determined or is inconstant, the leakage inductance should be designed as evenly distributed form in the respect of power efficiency. For the TAB converter which has fixed or symmetric power flow, the proposed design method has many advantages in terms of power efficiency, intrinsic decoupling control, cost, and etc.

Conclusion

The TAB converter can control each port power independently with two leakage inductances configuration. However, it decreases the power transfer efficiency in some power flow condition. In this paper, leakage inductance design procedure with a low leakage inductance at one port is suggested and compared with conventional configuration. In addition, the equations of peak inductor current are derived. In some power flow conditions, the peak current increases significantly. It leads to the increase of switching losses. Therefore, the position of low leakage inductance should be selected in consideration of power flow. To minimize the increase in turn-off switching loss, a low leakage inductance should be placed on the port that the delivers the most power of TAB converter.

References

[1] H. Tao, A. Kotsopoulos, J. L. Duarte and M. A. M. Hendrix.: Transformer-Coupled Multiport ZVS Bidirectional DC–DC Converter With Wide Input Range, IEEE Transactions on Power Electronics Vol. 23 no 2, pp 771-781

[2] J. Zeng, W. Qiao and L. Qu.: An Isolated Three-Port Bidirectional DC–DC Converter for Photovoltaic Systems With Energy Storage, IEEE Transactions on Industry Applications Vol. 51 no 4, pp 3493-3503

[3] Y. Chen, P. Wang, H. Li and M. Chen.: Power Flow Control in Multi-Active-Bridge Converters: Theories and Applications, 2019 IEEE Applied Power Electronics Conference and Exposition (APEC), pp. 1500-1507

[4] S. Bandyopadhyay, P. Purgat, Z. Qin and P. Bauer.: A Multi-Active Bridge Converter With Inherently Decoupled Power Flows, IEEE Transactions on Power Electronics Vol. 36 no. 2, pp 2231-2245

[5] L. F. Costa, G. Buticchi and M. Liserre.: Optimum Design of a Multiple-Active-Bridge DC–DC Converter for Smart Transformer, in IEEE Transactions on Power Electronics Vol. 33 no. 12, pp. 10112-10121

[6] S. Inoue and H. Akagi: A Bidirectional Isolated DC–DC Converter as a Core Circuit of the Next-Generation Medium-Voltage Power Conversion System, IEEE Transactions on Power Electronics, Vol. 22 no. 2, pp. 535-542

[7] F. Krismer and J. W. Kolar.: Accurate Power Loss Model Derivation of a High-Current Dual Active Bridge Converter for an Automotive Application, IEEE Transactions on Industrial Electronics, Vol. 57 no. 3, pp. 881-891

[8] H. Akagi, T. Yamagishi, N. M. L. Tan, S. -i. Kinouchi, Y. Miyazaki and M. Koyama.: Power-Loss Breakdown of a 750-V 100-kW 20-kHz Bidirectional Isolated DC–DC Converter Using SiC-MOSFET/SBD Dual Modules, IEEE Transactions on Industry Applications, Vol. 51 no. 1, pp. 420-428

[9] R. Haneda and H. Akagi.: Power-Loss Characterization and Reduction of the 750-V 100-KW 16-KHz Dual-Active-Bridge Converter With Buck and Boost Mode, IEEE Transactions on Industry Applications, vol. 58 no. 1, pp. 541-553